

**University of Massachusetts Amherst**

---

**From the Selected Works of Dimitrios Maroudas**

---

2009

# On the Hydrogen Storage Capacity of Carbon Nanotube Bundles

Dimitrios Maroudas, *University of Massachusetts - Amherst*

A. R. Muniz

M. Meyyappan



Available at: [https://works.bepress.com/dimitrios\\_maroudas/10/](https://works.bepress.com/dimitrios_maroudas/10/)

## On the hydrogen storage capacity of carbon nanotube bundles

Andre R. Muniz, M. Meyyappan, and Dimitrios Maroudas

Citation: *Appl. Phys. Lett.* **95**, 163111 (2009); doi: 10.1063/1.3253711

View online: <http://dx.doi.org/10.1063/1.3253711>

View Table of Contents: <http://apl.aip.org/resource/1/APPLAB/v95/i16>

Published by the [American Institute of Physics](#).

---

### Related Articles

Nanobubble clusters of dissolved gas in aqueous solutions of electrolyte. II. Theoretical interpretation  
*J. Chem. Phys.* **137**, 054707 (2012)

The effects of electronic polarization on water adsorption in metal-organic frameworks: H<sub>2</sub>O in MIL-53(Cr)  
*J. Chem. Phys.* **137**, 054704 (2012)

Computer simulation of adhesion between hydrophilic and hydrophobic self-assembled monolayers in water  
*J. Chem. Phys.* **137**, 054701 (2012)

Methane and carbon dioxide adsorption on edge-functionalized graphene: A comparative DFT study  
*J. Chem. Phys.* **137**, 054702 (2012)

Random sequential adsorption on fractals  
*J. Chem. Phys.* **137**, 044706 (2012)

---

### Additional information on Appl. Phys. Lett.

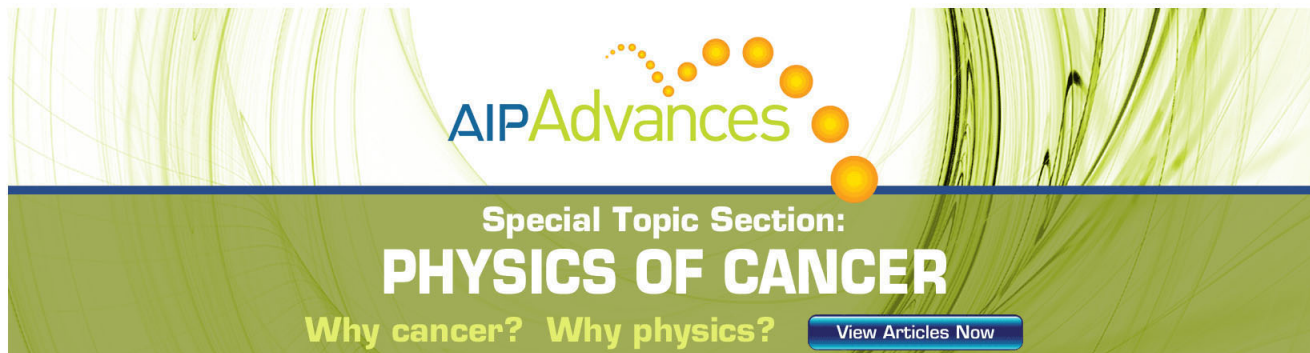
Journal Homepage: <http://apl.aip.org/>

Journal Information: [http://apl.aip.org/about/about\\_the\\_journal](http://apl.aip.org/about/about_the_journal)

Top downloads: [http://apl.aip.org/features/most\\_downloaded](http://apl.aip.org/features/most_downloaded)

Information for Authors: <http://apl.aip.org/authors>

## ADVERTISEMENT

The advertisement features a green background with abstract, flowing lines. At the top, the 'AIP Advances' logo is displayed, with 'AIP' in blue and 'Advances' in green, accompanied by a series of orange dots. Below the logo, the text 'Special Topic Section: PHYSICS OF CANCER' is written in white, with 'PHYSICS OF CANCER' in a larger, bold font. At the bottom, the phrase 'Why cancer? Why physics?' is written in yellow, and a blue button with the text 'View Articles Now' is located on the right side.

AIP Advances

Special Topic Section:  
**PHYSICS OF CANCER**

Why cancer? Why physics? [View Articles Now](#)

# On the hydrogen storage capacity of carbon nanotube bundles

Andre R. Muniz,<sup>1</sup> M. Meyyappan,<sup>2</sup> and Dimitrios Maroudas<sup>1,a)</sup>

<sup>1</sup>Department of Chemical Engineering, University of Massachusetts Amherst, Amherst, Massachusetts 01003-3110, USA

<sup>2</sup>Center for Nanotechnology, NASA Ames Research Center, Moffett Field, California 94035-1000, USA

(Received 11 September 2009; accepted 2 October 2009; published online 22 October 2009)

An analytical model is presented to describe the effect of carbon nanotube (CNT) swelling upon hydrogenation on the hydrogen storage capacity of single-walled CNT bundles; the model is properly parameterized using atomistic calculations for the relationship between CNT swelling and the degree of hydrogenation as measured by the coverage of the CNTs by chemisorbed atomic H. The model generates experimentally testable hypotheses, which can be used to explain the lower H storage capacities reported for CNT bundles and the experimentally observed nonuniformity of hydrogenation of CNT bundles. © 2009 American Institute of Physics. [doi:10.1063/1.3253711]

A massive body of experimental and theoretical work has investigated the hydrogen storage capacity of carbon nanotubes (CNTs) following the original demonstration that CNTs can be used as hydrogen storage media.<sup>1</sup> Storage capacities ranging from 0.25 to 20 wt % have been reported,<sup>2</sup> and numerous factors have been used to describe the variability and inconsistency of these results, including sample preparation, processing conditions, and presence of impurities such as amorphous carbon and catalyst particles. Both physisorption ( $H_2$ -CNT van der Waals interactions) and chemisorption (formation of stable  $sp^3$  C-H bonds) mechanisms have been accounted for hydrogen adsorption on CNTs. Chemisorption of H atoms (generated, e.g., in a  $H_2$  plasma) has been shown to provide storage capacities as high as 7 wt %, <sup>3-10</sup> close to the theoretical value of 7.7 wt %, corresponding to a CNT containing one chemisorbed H atom per C atom. The measured storage capacities based on this approach varied among different studies;<sup>3-10</sup> this discrepancy is also due to particular features of the sample used including CNT diameter distribution and bundle density<sup>9</sup> and source of H atoms.

A limiting factor in the potential hydrogen storage capacity using chemisorbed H is the structural change undergone by CNTs upon their hydrogenation. Theoretical<sup>11-17</sup> and experimental<sup>8,9</sup> studies have shown that hydrogenation causes CNT “swelling” as reflected by an increase in their dimensions. The resulting radial and axial strains are functions of the degree of hydrogenation as measured by the coverage,  $\Theta$ , of the nanotubes by chemisorbed atomic H.<sup>17</sup> When single-walled CNTs (SWCNTs) are in the form of bundles, the expansion of individual nanotubes upon hydrogenation may introduce certain complications in the efficient hydrogenation of the bundles. H atoms need to diffuse through the interstitial space of the bundle in order to reach the innermost tubes. This is illustrated in Fig. 1(a), where the simplest model of a bundle is depicted, consisting of a regular array of SWCNTs; the planar cross section of this array normal to the SWCNT axes forms a two-dimensional (2D) hexagonal lattice. The arrows in Fig. 1(a) denote the incoming atomic H flux. The hydrogenation-induced swelling of

the nanotubes leads to a decrease in the intertube spacing in the bundle; as a result, the diffusion of H atoms through this intertube space becomes more difficult. This mass-transfer limitation causes a nonuniformity of bundle hydrogenation and may limit the hydrogen storage capacity of the CNT bundles.

The purpose of this letter is to present an analytical model that describes the effect of nanotube swelling upon hydrogenation on the storage capacity of SWCNT bundles; the model is properly parameterized using atomistic calculations for the relationship between the relative increase on CNT dimensions and H coverage of the CNT. This model provides experimentally testable hypotheses which can be used to explain the observed storage capacities for bundles of SWCNTs.<sup>7,9,10</sup>

For a more detailed consideration of H mass transfer limitations in SWCNT bundles, we represent the bundle as a regular array of SWCNTs of equal diameter in their pristine state as depicted in Fig. 1(a). The only criterion that we employ for efficient H diffusion through carbon nanotubes in a bundle is a minimum intertube spacing,  $d_{\min}$ , requirement, i.e.,  $d \geq d_{\min}$ , is required for efficient H diffusion, where  $d$  is the intertube spacing. A close view of two nearest-neighbor nanotubes in the bundle is shown in Fig. 1(b). The corresponding geometrical relationship is  $2R(\Theta) + d(\Theta) = a$ , where  $R$  is the radius of the carbon nanotube,  $0 < \Theta \leq 1$ , and  $a$  is

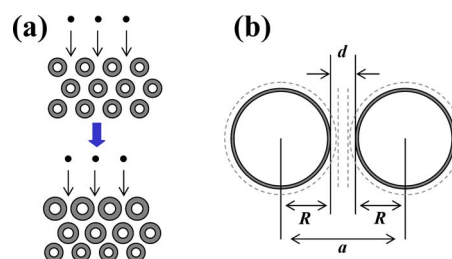


FIG. 1. (Color online) (a) Schematic of a SWCNT bundle exposed to an atomic H flux; the bundle is represented by a regular array of SWCNTs forming a hexagonal lattice on the plane normal to the SWCNT axes. The bundle is shown before (top) and after (bottom) its partial hydrogenation; the decrease in intertube spacing (bottom) is due to SWCNT swelling. (b) Characteristic dimensions of the bundle, namely, SWCNT radius,  $R$ , SWCNT center-to-center distance,  $a$ , and intertube spacing,  $d$ . The dashed lines are used to indicate deformation due to SWCNT swelling upon hydrogenation.

<sup>a)</sup>Author to whom correspondence should be addressed. Electronic mail: maroudas@ecs.umass.edu.

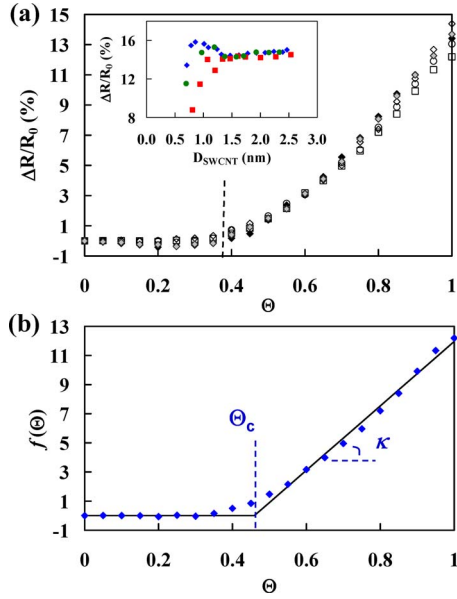


FIG. 2. (Color online) (a) Dependence on the H coverage  $\Theta$  of the radial strain  $\Delta R/R_0$  for the (24,0) (solid diamonds), (20,0) (gray diamonds), (15,0) (open diamonds), (9,9) (open squares), and (13,4) (open circles) SWCNTs. The inset shows the dependence of  $\Delta R/R_0$  on the pristine-SWCNT diameter for fully hydrogenated ( $\Theta=1$ ) zigzag (solid diamonds), chiral (solid circles), and armchair (solid squares) nanotubes; the chiral SWCNTs examined have chiral angles ranging from  $13.0^\circ$  to  $18.3^\circ$ . (b) Least-squares fitting of the swelling function  $f(\Theta) = \kappa(\Theta - \Theta_c)H(\Theta - \Theta_c)$  (solid line) to the atomistic-simulation results (discrete symbols) for the (9,9) SWCNT.

the lattice parameter of the 2D hexagonal lattice of Fig. 1(a);  $a$  is related to the density of the nanotube bundle,  $\rho_b$  [ $\rho_b = 2/(\sqrt{3}a^2)$ ]. The radius  $R$  accounts for the swelling of the individual nanotubes upon hydrogenation and can be expressed through a swelling function,  $f(\Theta)$ , as  $R(\Theta) = R_0[1 + f(\Theta)]$ , i.e.,  $f(\Theta) = \Delta R(\Theta)/R_0 \equiv [R(\Theta) - R_0]/R_0$  is the radial strain of the hydrogenated CNT, where  $R_0$  is the carbon nanotube radius in the pristine state,  $\Theta=0$ . Using  $d_{\min}$  as a characteristic length scale and introducing the dimensionless variables  $\delta \equiv d/d_{\min}$ ,  $\alpha \equiv a/d_{\min}$ ,  $\rho \equiv R/d_{\min}$ , and  $\rho_0 \equiv R_0/d_{\min}$ , the geometrical relationship becomes

$$\delta(\Theta) = \alpha - 2\rho_0[1 + f(\Theta)]. \quad (1)$$

The requirement for efficient H diffusion in the intertube space of the SWCNT bundle is  $\delta(\Theta) \geq 1$ . The actual numerical value of the characteristic length  $d_{\min}$  can be computed by atomistic simulations but it is not important for the present level of analysis.

The swelling function  $f(\Theta)$  is obtained by relaxing structures of pristine and hydrogenated SWCNTs of different diameters and chiralities at various coverages  $\Theta$  and calculating the resulting average  $R(\Theta)$ . Structural relaxation is based on isothermal-isobaric molecular-dynamics simulation using the adaptive intermolecular reactive empirical bonding order (AIREBO) potential<sup>18</sup> and following a procedure identical to that of Ref. 17 for H atoms distributed randomly on the SWCNT surfaces. Results for  $\Delta R(\Theta)/R_0$  are reported in Fig. 2(a) by averaging over an ensemble of five distributions for the following nanotube configurations: one armchair (9,9) (with diameter  $D=1.20$  nm at the pristine state), one chiral (13,4) ( $D=1.19$  nm), and three zigzag (15,0), (20,0), and (24,0) ( $D=1.16$ ,  $1.55$ , and  $1.85$  nm, respectively) SWCNTs. The trends observed are completely analogous to those re-

ported in Ref. 17:  $\Delta R(\Theta)/R_0$  is negligible at lower  $\Theta$ , but beyond a critical  $\Theta$ , it increases monotonically with  $\Theta$ ; at higher  $\Theta$ , this monotonic increase becomes linear.

The results of Fig. 2(a) show that for the smaller-diameter nanotubes [(9,9), (13,4), and (15,0) with  $D_{\text{average}} = 1.19$  nm],  $\Delta R(\Theta)/R_0$  depends on nanotube chirality only at higher  $\Theta$ . The results for the three zigzag nanotubes of different diameters show that  $\Delta R(\Theta)/R_0$  is practically independent of  $D$  within the range of diameters investigated. The dependence of  $\Delta R(\Theta)/R_0$  on diameter and chirality observed at high values of  $\Theta$  can be elucidated further by examining the dependence on  $D$  of  $\Delta R(\Theta=1)/R_0$ , i.e., for fully hydrogenated CNTs, as shown in the inset of Fig. 2(a). For smaller-diameter SWCNTs,  $\Delta R(1)/R_0$  depends on chirality, but for  $D > 1.3$  nm, the difference between the radial strains for SWCNTs of different chiralities is very small and the increase in  $\Delta R(1)/R_0$  with  $D$  is only very slight.

Next, we introduce the simplest possible parameterization of the swelling function  $f(\Theta)$ . This involves a Heaviside step function,  $H$ , and two parameters, the critical coverage,  $\Theta_c$ , for the onset of swelling and the slope  $\kappa$  of  $f(\Theta)$  in the linear regime, i.e., over the high- $\Theta$  range where the function  $f(\Theta)$  is linear. The corresponding analytical expression is  $f(\Theta) = \kappa(\Theta - \Theta_c)H(\Theta - \Theta_c)$ . The validity of this parameterization in approximating the actual computed swelling function is demonstrated in Fig. 2(b) through least-squares fitting of the analytical expression for  $f(\Theta)$  to the simulation results for  $f(\Theta)$  for the (9,9) SWCNT. The actual values of the parameters  $\kappa$  and  $\Theta_c$  depend on the diameters and chiralities of the carbon nanotubes. The least-squares estimates for the five sets of simulation results plotted in Fig. 2(a) are the following:  $(\kappa, \Theta_c) = (0.221, 0.459)$ ,  $(0.234, 0.461)$ ,  $(0.259, 0.480)$ ,  $(0.253, 0.471)$ , and  $(0.249, 0.465)$  for the (9,9), (13,4), (15,0), (20,0), and (24,0) SWCNTs, respectively. Finally, with this parameterization for  $f(\Theta)$ , Eq. (1) yields the criterion

$$\delta(\Theta) = \alpha - 2\rho_0[1 + \kappa(\Theta - \Theta_c)H(\Theta - \Theta_c)] \geq 1 \quad (2)$$

for efficient H diffusion in the carbon nanotube bundle.

Equation (2) can be used to investigate the dependence of  $\delta$  on the dimensionless lattice parameter  $\alpha$ , which is related to the bundle density  $\rho_b$ . In Fig. 3(a),  $\delta(\Theta)$  is plotted for  $\rho_0=4.0$ ,  $\kappa=0.240$ ,  $\Theta_c=0.470$ , and  $\alpha$  over the range  $9.1 \leq \alpha \leq 10.3$ . From this plot, it is evident that for dense bundles (low values of  $\alpha$ ), the criterion  $\delta > 1$  is satisfied for  $\Theta$  lower than a critical value. Considering that the outermost tubes are the first ones to be hydrogenated, this critical value of  $\Theta$  corresponds to the maximum degree of hydrogenation that can be achieved for the innermost tubes of the bundle. For the densest bundles represented in this figure, the extent of hydrogenation is only 50%. For more dispersed bundles (higher values of  $\alpha$ ), the maximum possible degree of hydrogenation (before  $\delta$  decreases to its critical value of one), increases with increasing  $\alpha$ . If the nanotubes are dispersed enough, the H mass-transfer limitations are eliminated and the maximum storage capacity of the nanotube bundles can be achieved. However, increasing  $\alpha$  causes a decrease in  $\rho_b$  and increases the footprint of the storage media for a given storage capacity; the relationship  $\rho_b \propto 1/a^2$  is depicted in the inset of Fig. 3(a). Figure 3(b) shows that the maximum degree of hydrogenation realized may also depend on the atomic-scale characteristics of the nanotubes, namely, their



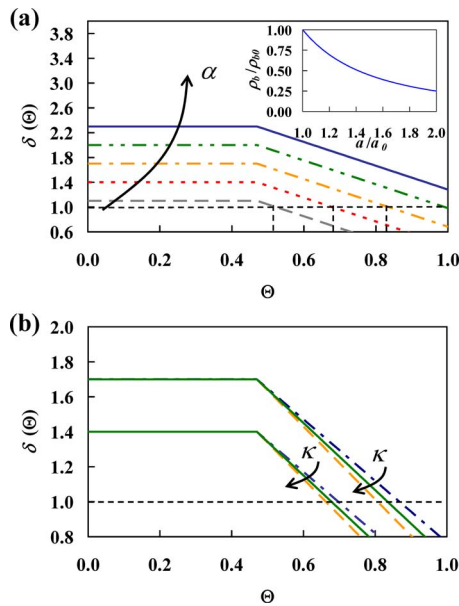


FIG. 3. (Color online) (a) Dimensionless intertube spacing  $\delta$  as a function of  $\Theta$  and its variation with the bundle density, as expressed by the dimensionless lattice parameter  $\alpha$ . The lines shown correspond to  $\alpha=9.1$ , 9.4, 9.7, 10.0, and 10.3. The inset shows the decrease of the bundle density as the lattice parameter increases; both quantities are made dimensionless with their values at the pristine state,  $\Theta=0$ . (b)  $\delta$  as a function of  $\Theta$  for two bundle densities and its dependence on nanotube diameter or chirality, as expressed by the dimensionless parameter  $\kappa$ . The different lines in the two sets correspond to  $\kappa=0.22$ , 0.24, and 0.26.

chiralities and diameters. For example, the variation of the parameter  $\kappa$ , which is determined by the SWCNT chirality and diameter, results in different ranges of  $\Theta$  which satisfy the criterion  $\delta(\Theta) > 1$ ; in Fig. 3(b), we used two values of  $\alpha$  ( $\alpha=9.4$  and  $\alpha=9.7$ ),  $\Theta_c=0.47$ ,  $\rho_0=4.0$ , and three representative values of  $\kappa$  ( $\kappa=0.22$ , 0.24, and 0.26). By comparing the two cases, it is evident that for denser bundles the effects of SWCNT chirality and diameter are less pronounced than those for more dispersed bundles.

The swelling effect on individual nanotubes that our model considers has been studied before<sup>11,12</sup> and indicated the possibility of 100% coverage with half of the hydrogen inside and half outside the nanotubes. However, here we have studied the effect for a more practical configuration of nanotube bundles by considering mass transfer limitations for the atomic hydrogen flux to reach the innermost tubes inside a bundle. A major implication of the model is that proper tailoring of the bundle density will improve the H storage capacity of carbon nanotubes substantially; this can be accomplished by lowering the bundle density to an optimal value that increases the degree of hydrogenation to  $\Theta=1$ . In addition, the criterion of Eq. (2) is experimentally testable and provides a possible explanation for the observed storage capacities lower than 100% that have been reported in experiments.

Finally, we discuss our findings in the context of the experimental results. Ruffieux *et al.*<sup>5</sup> reported a saturation in

H uptake after 200 s, leveling off at 50% capacity. Nikitin *et al.*<sup>7</sup> exposed several films of SWCNTs to an atomic hydrogen beam and measured storage capacities of 65% and of 30% and close to 100%.<sup>9</sup> In Ref. 9, the storage capacity of  $\sim 100\%$  of the second sample was achieved in the outermost nanotubes of the film and the hydrogenation of the sample was nonuniform; hydrogenation was practically uniform through the film for degrees of hydrogenation up to  $40 \pm 5\%$ . These results are consistent with our model predictions, including the predicted values of  $\Theta_c$  ( $\sim 45\%$ ). The lowest reported hydrogen uptake is 20% for a 13- $\mu\text{m}$ -tall tower of SWCNTs grown on a silicon substrate.<sup>10</sup> According to our model, it is expected that, in this case, the degree of hydrogenation is low due to the very high density of the vertically aligned nanotubes in the tower and the associated difficulty for the atomic hydrogen flux to reach the nanotube surfaces at the bottom of the tower.

Our theoretical study shows how to circumvent mass transfer limitations in order to maximize the hydrogen storage capacity of SWCNT bundles and obtain a 7.0–8.0 wt % storage through atomic H chemisorption. However, practical considerations demand a careful evaluation of the energy penalty associated with the production of H atoms using a plasma or an atomic beam, particularly relative to *in situ* catalytic dissociation of  $\text{H}_2$ . Recent advances in atmospheric plasmas may offer an avenue to reduce this energy penalty.

This work was supported by the National Science Foundation through Grant Nos. CMMI-0531171 and CBET-0613501 and by a CAPES/Fulbright Fellowship to A.R.M.

- <sup>1</sup>A. C. Dillon, K. M. Jones, T. A. Bekkedahl, C. H. Kiang, D. S. Bethune, and M. J. Heben, *Nature (London)* **386**, 377 (1997).
- <sup>2</sup>Y. Yürüm, A. Taralp, and T. N. Veziroglu, *Int. J. Hydrogen Energy* **34**, 3784 (2009), and references therein.
- <sup>3</sup>B. N. Khare, M. Meyyappan, A. M. Cassell, C. V. Nguyen, and J. Han, *Nano Lett.* **2**, 73 (2002).
- <sup>4</sup>B. N. Khare, M. Meyyappan, J. Kralj, P. Wihite, M. Sisay, H. Imanaka, J. Koehne, and C. W. Bauschlicher, Jr., *Appl. Phys. Lett.* **81**, 5237 (2002).
- <sup>5</sup>P. Ruffieux, O. Gröning, M. Biemann, P. Mauron, L. Schlapbach, and P. Gröning, *Phys. Rev. B* **66**, 245416 (2002).
- <sup>6</sup>P. Ruffieux, O. Gröning, M. Biemann, and P. Gröning, *Appl. Phys. A: Mater. Sci. Process.* **78**, 975 (2004).
- <sup>7</sup>A. Nikitin, H. Ogasawara, D. Mann, R. Denecke, Z. Zhang, H. Dai, K. Cho, and A. Nilsson, *Phys. Rev. Lett.* **95**, 225507 (2005).
- <sup>8</sup>G. Zhang, P. Qi, X. Wang, Y. Lu, D. Mann, X. Li, and H. Dai, *J. Am. Chem. Soc.* **128**, 6026 (2006).
- <sup>9</sup>A. Nikitin, X. Li, Z. Zhang, H. Ogasawara, H. Dai, and A. Nilsson, *Nano Lett.* **8**, 162 (2008).
- <sup>10</sup>A. Tokura, F. Maeda, Y. Teraoka, A. Yoshigoe, D. Takagi, Y. Homma, Y. Watanabe, and Y. Kobayashi, *Carbon* **46**, 1903 (2008).
- <sup>11</sup>C. W. Bauschlicher, *Nano Lett.* **1**, 223 (2001).
- <sup>12</sup>C. W. Bauschlicher and C. R. So, *Nano Lett.* **2**, 337 (2002).
- <sup>13</sup>T. Yildirim, O. Gulseren, and S. Ciraci, *Phys. Rev. B* **64**, 075404 (2001).
- <sup>14</sup>O. Gulseren, T. Yildirim, and S. Ciraci, *Phys. Rev. B* **66**, 121401 (2002).
- <sup>15</sup>M. Volpe and F. Cleri, *Surf. Sci.* **544**, 24 (2003).
- <sup>16</sup>K. A. Park, K. Seo, and Y. H. Lee, *J. Phys. Chem. B* **109**, 8967 (2005).
- <sup>17</sup>A. R. Muniz, T. Singh, and D. Maroudas, *Appl. Phys. Lett.* **94**, 103108 (2009).
- <sup>18</sup>S. J. Stuart, A. B. Tutein, and J. A. Harrison, *J. Chem. Phys.* **112**, 6472 (2000).